Raul Sanchez
e-mail: raul.sanchez@upm.es

Luis Juana
e-mail: luis.juana@upm.es

Departamento de Ingenierfa Rural.
Technical University of Madrid (UPM).
ETSI Agronomos.
Ciudad Universitarias/n.
Madrid 28040, Spain

Francisco V. Laguna
Departamento de Ingenierfa Civil: Hidraulica y Energetica.
Technical University of Madrid (UPM).
ETSI Caminos.
Canalesy Puertos.
C/Profesor Aranguren s/n
Madrid 28040, Spain
e-mail: he15@caminos.upm.es

Leonor Rodrfguez-Sinobas
Departamento de Ingenierfa Rural.
Technical University of Madrid (UPM).
ETSI Agronomos.
Ciudad Universitarias/n.
Madrid 28040, Spain
e-mail: leonor.rodriguez.sinobas@upm.es

Estimation of Cavitation Limits From Local Head Loss Coefficient

Cavitation effects in valves and other sudden transitions in water distribution systems are studied as their better understanding and quantification is needed for design and analysis purposes and for predicting and controlling their operation. Two dimensionless coefficients are used to characterize and verify local effects under cavitating flow conditions: the coefficient of local head losses and the minimum value of the cavitation number. In principle, both coefficients must be determined experimentally, but a semianalytical relationship between them is here proposed so that if one of them is known, its value can be used to estimate the corresponding value of the other one. This relationship is experimentally contrasted by measuring head losses and flow rates. It is also shown that cavitation number values, called cavitation limits, such as the critical cavitation limit, can be related in a simple but practical way with the mentioned minimum cavitation number and with a given pressure fluctuation level. Head losses under conditions of cavitation in sharp-edged orifices and valves are predicted for changes in upstream and downstream boundary conditions. An experimental determination of the coefficient of local head losses and the minimum value of the cavitation number is not dependent on the boundary conditions even if vapor cavity extends far enough to reach a downstream pressure tap. Also, the effects of cavitation and displacement of moving parts of valves on head losses can be split. A relatively simple formulation for local head losses including cavitation influence is presented. It can be incorporated to water distribution analysis models to improve their results when cavitation occurs. Likewise, it can also be used to elaborate information about validity limits of head losses in valves and other sudden transitions and to interpret the results of head loss tests.

Keywords: local head losses, cavitation, valve, orifice, pipeline design

Introduction

As dictated by Bernoulli's equation, there is a drop in the pressure of the permanent regime flow in a constriction, such as a valve, due to increased velocity. The phenomenon of cavitation can materialize if the pressure drop is big enough. It is also known that local head losses take place primarily in the expansion, characterized by the presence of vortices, which exist in the turbulent wake, downstream of the point of flow separation. In addition vortices contain regions of high velocity and hence low pressure. These areas of low pressure are potential sites for vapor formation.

Cavitation reduces a device's flow capacity, or, concurrently, head losses are greater as the more intense cavitation is. Tullis set out several definitions of cavitation limits according to observable effects on flow. These limits include the choking cavitation limit, from which cavitation affects the flow capacity of a device. Unless this limit is reached, even if cavitation takes place, the effects of this phenomenon on head losses are practically negligible and scale effect is appreciated (Ball and Tullis , Tullis). Similarly, Testud studied experimentally the noise generated by a single hole and a multihole sharp-edged orifice, both with the same cross-sectional opening, in a water pipe. They concluded that below the choking cavitation limit the multihole is more silent than the single hole orifice. Also, it can be observed in the experimental results that the head loss coefficient and the choking cavitation limit are equivalent in both, indicating that the distribution of cross-sectional opening should not have any effect on these two coefficients.

Zhang and Cai studied experimentally the geometric shape of orifices that produce the same head loss with the aim of reducing the pressure drop associated with the cavitation risk. Similarly, Zhang and Chai [6] indicated the importance of quantifying cavitation in energy dissipation hydraulic works and, particularly, when examining a serial arrangement of orifices to achieve this goal. In this respect, there is a complementary wide technical literature, such as ANSI/ISA and Idel'cik , which compiled many particular empirical studies about head losses and cavitation, in general without relation to each other.

From experimental determinations, the choking cavitation limit for sharp-edged orifices is a function of geometric parameters only, and the effect of the scale is negligible (Tullis , Tullis and Govindarajan). Mishra and Peles also reached the same conclusion again for orifices. In this last paper, they examined the size-dependent similarities and differences in cavitation, for which purpose they use orifices measuring from just a few micrometers to several centimeters. Additionally, as head losses are also dependent on the geometric shape, it is possible to get an analytical relationship between the head loss coefficient and the choking cavitation limit in relatively simple sudden transitions, as shown by Sarpkaya and Nurick . In the last two papers, the flow has been characterized by means of the contraction coefficient.

One of the objectives of this paper was to predict the head losses in a sudden transition for any boundary condition imposed by the distribution system and especially in cases with uncertainty about the cavitation impact on such head losses. In principle, two independent coefficients, one for head losses and another for cavitation, should suffice to characterize a particular transition and

achieve the objective. On the other hand, information about head losses in valves and other singular elements is relatively extensive. However the one concerned on cavitation is scarce. Thus, it is worthwhile to estimate the cavitation-related coefficient from the head loss coefficient.

Additionally, the elements of valves are subject to drag force. On top of the possible variability of head losses due to the displacement of their closing elements are losses induced by the potential impact of cavitation. By predicting head losses under circumstances in which they are significantly affected by cavitation, it will be possible to separate cavitation effect and, consequently, to specify what effects the above displacement has on head losses and draw conclusions about the behavior of such control devices.

Finally, the presence of cavitation does not imply a significant effect on head losses, but other unwanted effects, such as noise, vibration, and erosion damage, can be found. Therefore, another objective of this paper is to develop a procedure for estimating a value of the cavitation number for use as a reference against which to compare and to determine other cavitation limits.

Materials and Methods

The hydraulics general equation for the study of local head losses *he* in transitions can be expressed as

$$h_f = K\left(\frac{III}{l'}, \frac{l}{l''}, \ldots, \mathrm{Re}, \ldots\right)\frac{U^2}{2g} \qquad (1)$$

As the length of a transition is relatively short, friction-induced head losses are negligible as compared with separation-induced losses. Additionally, rapidly varied flow in a transition between straight cross-sections with uniform movement is often considered in practice to be given in terms of fully developed turbulence. Then, the Reynolds number Re is not part of the local head loss coefficient *K,* and this only depends on the relations between the geometric dimensions *I, V, I".* This way, local head losses in any given geometric shape are characterized by a constant coefficient *K.*

In a transition with identical sections at each end and disregarding the differences of elevation between their centroids, the coefficient is determined by

$$K = \frac{P1-P2}{U^2} \qquad (2)$$

Subindex 1 refers to section 1 immediately upstream of the transition, and 2 refers to the downstream section 2. p is the water density, *U* is the mean flow velocity determined from the reference section, generally the nominal section, and *(p\-pi)* is the pressure difference between the section immediately upstream of the transition and the downstream section in which the regime returns to uniform.

Because of the fact that for constant flow rate, head losses are greater the more intense cavitation is, the minimum value K_m of the dimensionless local head loss coefficient has been used when cavitation has no influence on head losses.

Besides, the dimensionless cavitation number ***a*** is used to characterize the phenomenon of cavitation. Batchelor showed this parameter, in its general form, as the pressure over vapor pressure/ velocity head. In particular, for either the upstream or the downstream sections, this parameter is expressed as

$$\frac{Pi-Pv}{U^1} \qquad \frac{P1-P2+P2-P,}{U^1} \qquad K+\frac{Pl-Pv}{U^2} \quad \bullet K+a_2 \qquad (3)$$

Another way of expressing the parameter *a,* often used in research looking at cavitation in internal flows, is to divide by the

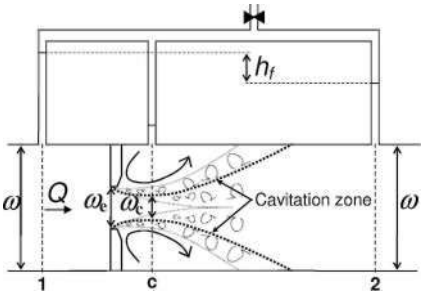

Fig. 1 Cavitating region downstream a sharp-edged orifice and piezometric levels indicated by a differential air manometer

$$\sigma_{p1} = \frac{\sigma_1}{K} = \frac{p_1 - p_v}{p_1 - p_2} = \frac{p_1 - p_2 + p_2 - p_v}{p_1 - p_2} = 1 + \frac{p_2 - p_v}{p_1 - p_2}$$

$$= 1 + \sigma_{p2} = 1 + \frac{\sigma_2}{K} \qquad (4)$$

<*j* is a parameter that characterizes the system-imposed pressure boundary conditions. If the pressure in section 2 were equal to the vapor pressure, there would be a vapor filled cavity stretching at least as far as that section. In this case, $<r_{p2}$ would be equal to zero, or the equivalent cr_{pl} would be equal to 1.

In short, *K* characterizes head losses as ***a*** does for system-imposed boundary conditions. When cavitation has influence on head losses, they are related. Thus, we have proposed a relationship between them, at first for sharp-edged orifices, in which upstream head losses can be neglected in comparison with downstream ones. Secondly, the relationship for transitions such as sharp-edged orifices have been modified to extend it to general transitions, such as valves.

Sharp-Edged Orifices. Flow expressions for sharp-edged orifices were obtained by considering friction head losses negligible, so they are due exclusively to separation effects and, therefore, are concentrated where the streamlines are divergent (see the diagram in Fig. 1). Thus, the losses between sections 1 and c were neglected, as the streamlines in this region are convergent, and only the losses that take place in the flow expansion between c and 2 were considered.

On the other hand, the continuity equation was expressed as

$$Q = U \bullet o) = U_c \bullet o)_c = U_c \bullet C_c \bullet o)_e \qquad (5)$$

where *U* is the mean water velocity in section *to* and U_c is the mean water velocity in the contracted jet section to_c. This latter section is usually expressed as the product of the orifice section to_e multiplied by the contraction coefficient C_c. This latter is a classic coefficient in hydraulics, which is dimensionless and is related to the ratio between the section immediately upstream of the orifice and the orifice section.

Bearing in mind that the head losses between sections 1 and c are negligible, the difference between the respective pressure heads is exclusively a function of the difference between the velocity heads. Therefore, taking into account Eq. (5), flow discharge expressed as a function of the pressure difference is

$$Q = \frac{\sqrt{Pl-Pc}}{\frac{p}{2}\sqrt{\left(\frac{M}{(C_c-o)J}\right)^2 - 1}} \qquad (6)$$

From the comparison between Eqs. (6) and (3) and Eq. (3), it can be found that when cavitation occurs in section c with intensity enough for p_c to lessen and approximately reach p_v, the value of crj is minimum (cr_{lm}), and this latter is a function of geometric

parameters only. It can be equated to the choking cavitation limit. For the sharp-edged orifice in question, this limit is

$$\sigma_{1m} = \left(\frac{\omega}{C_c \cdot \omega_e}\right)^2 - 1 \quad (7)$$

Due to the nature of C_c mentioned above, the coefficient cr_{lm} characterizes the flow pattern upstream of the contracted section c.

To study the cavitation influence on head losses, the flow rate Q has been expressed as a function of these, which are related to the pressure head difference between the two end sections of the transition. Thus, head losses need to be included. Belanger-Borda's expression, in which head losses are related to the square of the difference between velocities, is useful when considering that head losses occur exclusively at the flow expansion between sections c and 2. Moreover, together with the continuity (Eq. (5)), they can be expressed as

$$h_f = H_1 - H_2 = \frac{p_1 - p_2}{\gamma} \approx H_c - H_2 = \frac{(U_c - U)^2}{2g} = \left(\frac{\omega}{C_c \cdot \omega_e} - 1\right)^{\tilde{}\wedge 2} 2g = K_m \frac{U^2}{2g} \quad (8)$$

Note that K_m depends only on just the geometric parameters, as was the case for <r_lm. Moreover, under the assumption of friction-induced head losses being negligible, it characterizes the flow pattern downstream of section c, unlike <r_lm, which characterized the flow pattern upstream. Our proposal is that these two parameters, K_m and <r_lm, should characterize a transition to simulate and predict head losses under cavitation conditions.

From Eqs. (5) and (8), flow can be expressed as

$$Q = \omega \sqrt{\frac{p_1 - p_2}{\frac{\rho}{2}\left(\frac{\omega}{C_c \cdot \omega_e} - 1\right)^2}} = \omega \sqrt{\frac{p_1 - p_2}{\frac{\rho}{2} K}} \quad (9)$$

From the elimination of Q from Eqs. (6) and (9), it is inferred that $P2 > P_C$ because $C_c \bullet to_e < to$. Additionally, due to the constraint that within tap water (with nuclei), the pressure cannot fall below its vapor pressure p_v, the flow (Eq. (9)) will be valid only if $p_c > p_v$. When this limit materializes in section c, flow will be conditioned by cavitation. This latter is denoted by Q_v, which is obtained by substituting p_c by p_v in Eq. (6), giving

$$\&= \omega \sqrt{\frac{p_1 - p_v}{\frac{\rho}{2}\left[\left(\frac{\omega}{C_c \cdot \omega_e}\right)^2 - 1\right]}} = \omega \sqrt{\frac{p_1 - p_v}{\frac{\rho}{2}\sigma_{1m}}} \quad (10)$$

Notice that under the above stated conditions flow depends on p_x only.

In conclusion, in cases with the head losses upstream of section w_c being negligible and with the downstream flow pattern following a sudden expansion from the contracted section ($o_c = C_c\ to_e$, the coefficients K_m and <r_lm are related. The relationship in question can be obtained by eliminating the ratio between to_c and C_c (o_e from expressions of <r_lm and K in Eqs. (7) and (8), respectively, as follows:

$$\sigma_{1m} = K_m + 2\sqrt{K_m} \quad (11)$$

Valves. Valves are geometric transitions more complex than sharp-edged orifices. In the case of a nonaxisymmetric flow pattern, a conclusion in Rouse and Jezdinsky's [15] paper is that measurements of cavitation and pressure fluctuation made under conditions of axial symmetry should not be applied quantitatively. Besides, some particularities of flow inside valves must be borne in mind. First, it could be possible that downstream of the closing element of a valve, a cross jet section with uniform flow would not occur. So then, an energy conservation equation could not be applied between sections with nonuniform flow. Second, head losses could not adapt precisely to a sudden expansion. Even so, and being less precise than for circular orifices, it is worthwhile to formulate an approximate expression for studying in a general way a great number of possible specific cases. Thus, the relation between the coefficients K_m and <r_lm can also be approximated as follows. In essence, a part of the head losses will also take place in the expansion downstream of the regions in which the flow is contracted, where the streamlines are divergent, and $o)_c$ has been used for the equivalent contracted section that would produce such losses in a sudden expansion, such a what occurs downstream a sharp-edged orifice. In a manner akin to the way in which K_m was represented in Eq. (8), the corresponding head loss coefficient is now expressed as

$$K_m = \left(\frac{\omega}{U_{\tilde{}}} 1\right)^2 \quad (12)$$

In contrast, with respect to cavitation, because flow in the region where the streamlines are convergent will not be axisymmetric either, velocity distribution in the contracted jet section will be more dispersed than in the axisymmetric flow, and cavitation could now appear at particular locations under less severe conditions. Therefore, bearing in mind the above mentioned particularities, the equivalent contracted section to_c has been corrected with coefficient r, which is positive and less than 1 and is characteristic of every geometric shape. This coefficient attempts to take into account the mentioned particularities. As shown in Eq. (7) for sharp-edged orifices, <r_lm is a function of the geometric parameters and is now expressed as

$$\sigma_{1m} = \left(\frac{\omega}{r \cdot \omega_e}\right)^2 \text{"} 1 \quad (13)$$

Eliminating the ratio between the nominal and the equivalent contracted section from Eqs. (12) and (13), a relationship between K_m and <r_lm can be obtained. Furthermore, on top of the head losses in the expansion from the contracted region induced by the closing element of valves, there are losses caused by separation effects inside the body of such valves. Denoting the coefficient that quantifies the closing element-independent upstream losses as K_0, already included in K_m, the relation between K_m and <r_lm is now expressed as

$$\sigma_{1m} = \frac{1}{r^2}(\sqrt{K_m - K_0} + 1)^2 - 1 \quad (14)$$

The coefficient K_0 will be small or even zero in valves in which head losses are relatively low when they are fully open, as can be the case with butterfly valves. For other valve types, in the absence of specific studies, the value of the coefficient K_m for a valve that is in a completely open position could be considered to approximate K_0 (more details about K_0 and head losses for seat valves can be found in Sanchez [16]). The value of r is harder to approximate than K_0 and is therefore only studied experimentally in this paper.

Application. If the parameters K_m and <r_lm are known, either the head losses or the flow can be obtained from the system-imposed boundary conditions. These conditions are characterized by the cavitation number $\boldsymbol{a}$ in its forms <T_2 and a_{p2} shown in Eqs. (3) and (4).

Thus, Eqs. (9) and (10) for flow rate Q can be generally expressed, under both cavitating and noncavitating conditions, as a function of the pressure difference between the sections upstream and downstream of the singularity, $P\text{-}p_2$, or the head losses ht, with

$$Q = \omega \sqrt{\frac{p_1 - p_2}{\frac{\rho}{2} K}} = \omega \sqrt{\frac{2 \cdot g \cdot h_f}{K}} \quad (15)$$

where K is the only coefficient that has to be evaluated. This can

be achieved with the function detailed below.

The value of K can be obtained from the value of the cavitation number in its forms a_2 (if p_2 and U—or Q—are known) and a_{p2} (if p_2 and/?! are known). In the first case, if $0=Scr_2=Scr_{2v}$, this last being equal to $a^{\wedge}{}_m$—K_m, there would be cavitation and it would affect the head losses. If $cr_2>cr_{2v}$, either there would be no cavitation or there would be but it would not affect the head losses. In either case, coefficient K would be given by

$$K\begin{cases} 0 \le \sigma_2 \le \sigma_{2v} \rightarrow K = \dfrac{p_1 - p_2}{\rho\dfrac{U^2}{2}} = \dfrac{p_1 - p_v - (p_2 - p_v)}{\rho\dfrac{U^2}{2}} = \sigma_{1m} - \sigma_2 \ge K_m \\ \sigma_2 > \sigma_{2v} \rightarrow K = K_m \end{cases} \tag{16}$$

$$K\begin{cases} 0 \le \sigma_{p2} \le \sigma_{p2v} = \dfrac{\sigma_{1m}}{K_m} - 1 \rightarrow K = \dfrac{p_1 - p_2}{\rho\dfrac{U^2}{2}} = \dfrac{p_1 - p_2}{p_1 - p_v} \cdot \sigma_{1m} = \dfrac{\sigma_{1m}}{1 + \sigma_{p2}} \ge K_m \\ \sigma_{p2} > \sigma_{p2v} \rightarrow K = K_m \end{cases} \tag{17}$$

On the other hand, if the loop flow correction method of network analysis is used, in which flow rates are corrected to fulfil energy equations, then Eq. (16) solves the problem. However, the value of p_2 is necessary and can be obtained from the previous iteration.

In spite of the fact that cr_1 can be used instead of $<r_2$, it is useful to determine the latter to quantify the head losses increased by cavitation and to compare qualitatively the possible lengthening of the vapor cavity. While $<r_{lm}$ is the minimum value of cr_1, which is reached when the pressure in the contracted section is equal to p_v, the minimum value of a_2 is zero (when $p_2=p_v$), ^{an}d cavitation materializes its effects on head losses when $cr_2=Scr_{2v}$. So, a_2 gives more information than cr_1.

To illustrate the utility of Eqs. (15) and (16), a system such as that shown in Fig. *2(a)* has been considered. The system boundary conditions are imposed by the tank levels. Additionally, if the head losses in the pipes upstream and downstream of the valve V are considered negligible, the pressures resulting from the above boundary conditions can also be considered in the sections immediately upstream and downstream of that valve. The coefficient K has been calculated using Eq. (17) for each situation imposed on the system, which is characterized by the parameter a_{p2}.

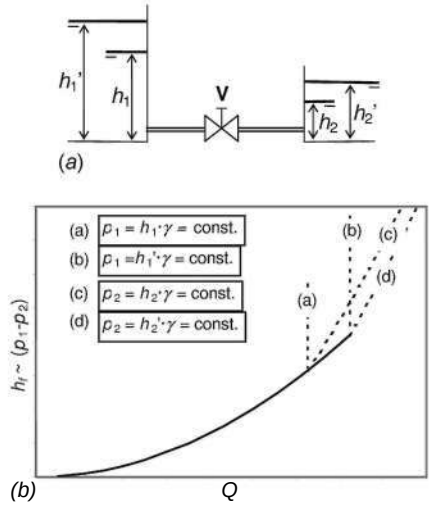

Fig. 2 (a) Valve between two tanks, *(b)* Head losses as a function of flow under different system-imposed boundary conditions.

Figure *2(b)* shows the possible shapes of the curves plotting the head losses in the valve V, or other transition, as a function of flow rate for different boundary conditions indicated in Fig. *2(a).* Curves (a) and (b) match permanent flow regime situations where the water level in the upstream tank is constant, whereas the downstream pressure changes. The opposite applies to curves (c) and (d), and the water level in the downstream tank is constant, whereas the upstream pressure changes. All four curves have a common section, depicted as a solid line, in which the cavitation effects do not affect head losses. This is compatible with situations in which $K=K_m$.

Additionally, where $a\text{-}_{pl}{}^{\wedge}cr_{lm}/K_m$ or $a\text{-}_{p2}{}^{\wedge}cr_{lm}/K_m\text{-}l$, cavitation effects affect head losses, the value of K depends on the value of cr_pi, and, therefore, the relations between head losses and the flow rate differ depending on the boundary condition, which is changed. It can be seen that if $p\backslash$ is constant, then Q is too, irrespective of the value of p_2, which conforms to Eq. (10). This also applies when p_2 is constant and p_1 changes. Under these conditions, Q is a function of p_1.

In a real system, because head losses in upstream and downstream pipes cannot be considered negligible, the hypothetically observed lines would be positioned in-between the dashed plotted curves. Therefore, the representation of *hJQ)* is inadequate for determining the parameters that quantify cavitation effects on head losses. However, the one of $K(cr_1)$ represents the head losses irrespective of the operation of the rest of the system components, and it should then be an effective tool for determining such parameters.

Experimental Verification. The above mentioned developments have been verified experimentally. We tested the following devices: three 7.56 mm, 8.93 mm, and 11.59 mm circular sharp-edged orifices, a butterfly valve with a nominal diameter of 75 mm and a symmetric closing disk, and a hydraulically operated seat globe valve with a nominal diameter of 50 mm. The orifices were positioned in transparent methacrylate (see Fig. 3) and opaque polyvinyl chloride (PVC) pipes with internal diameters of 16 mm and 16.2 mm, respectively. The two valves were positioned in their respective PVC pipes with the same nominal diameters.

All the listed devices were arranged in a test rig. Figure 4 is a

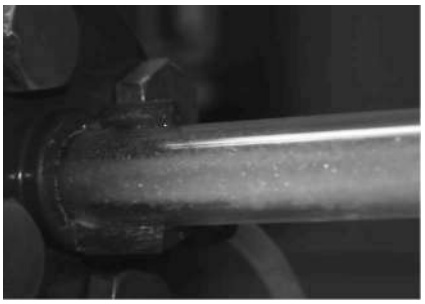

Fig. 3 View of cavitating flow downstream of one of the tested sharp-edged orifices

simplified diagram of the test rig. The diagram represents a closed circuit whose storage element is tank T and the energy comes from pump P, driven by a frequency converter-controlled electric motor.

The measurement equipment was composed of the next elements. The electromagnetic flowmeter F was used to measure flow, a digital differential manometer M_2 was used to measure the head losses in the tested elements V, and the digital manometer M_1 was used to measure the upstream pressure. Pressure h_2 was calculated as the difference between h_1 and ht, measured by M_t and M_2, respectively.

The distances between the element under testing and the measurement and control elements L_u L_2, L_3, and L_4 in Fig. 4 conformed to ISA and ASAE instructions. In particular, L_2 and L_3 were equal to one and five times internal pipe diameters, respectively, while L_1 and L_4 were greater than ten and two times this diameter.

The control of the boundary conditions during the tests was achieved as follows. The upstream boundary condition was controlled by valves V_r and V_1; the above frequency converter, and a combination of any of these elements. Because valves affect the uniformity of flow downstream of them, it was done almost exclusively using the frequency converter. The only way to control the downstream boundary condition was to actuate on valve V_2.

The upstream and downstream boundary conditions of the element under testing, V, were relations between the pressure heads hi and h_2, respectively, and flow Q. For predicting head losses in the tested element under the particular conditions imposed in the test rig, these last ones in a permanent regime have been modeled by the following two equations:

$$h_1 = a_0 \cdot N^2 + a_1 \cdot N \cdot Q + a_2 \cdot Q^2 \tag{18}$$

$$Q = C_D \sqrt{h_2 - \Delta z} \tag{19}$$

Equation (18) is a standard expression for pumping head characteristic curves and is applicable in this case if V_r is closed. N represents the relation between the real frequency provided by the converter and the nominal frequency of the motor that drives the pump. The coefficients a_0, a_1; and a_2 were obtained by fitting. The last two coefficients appear to account for the head losses in the pipes making up the upstream section, whereas the first coefficient gives the pressure head with zero flow.

As regards the downstream section, the coefficients C_D and Az

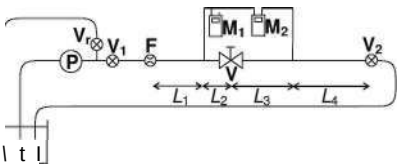

Fig. 4 Hydraulic schematic diagram of the test rig

of Eq. (19) were also obtained by fitting. In physical terms, the second coefficient means the height difference between the free water level in tank T and the section at which h_2 is measured. C_D covers the head losses in both V_2 and the downstream pipes, assuming a full turbulence regime. Additionally, if the vapor cavity extends to the downstream manometer tap, the approximate boundary value of the measure here would be p_v, and then this boundary condition would *be* $p_2 \sim p_v$.

As far as the test procedure is concerned, the above devices were tested under constant downstream and upstream discharge conditions. In the first case, valve V_2 was fixed in a fully open position. This way we were able to model this condition using Eq. (19), unless the vapor cavity had, due to its extension, affected the measurements of p_2. In the case of the fixed upstream condition, the tests were run with valve V_r at a closed position, \1 at a fully open position, and pump P at a constant rotation regime. All the tests were run with tap water contained in tank T at a temperature of approximately 20 °C, and the absolute vapor pressure at the saturation point considered was 2.4 kPa. As observed experimentally by Tullis and Skinner , air injection downstream the valves reduces the critical cavitation index and the magnitude of the low frequency pressure fluctuations but not the local head loss coefficient, so the presence of small quantities of dissolved or undissolved air in water should not affect the determinations of either the last mentioned coefficient or the choking cavitation index.

Also, the closing elements of valves were subject to the force generated by the fluid. As Sarpkaya had observed and analyzed, the drag force on the round disk of an axisymmetric butterfly valve generates a torque that tends to close the valve.

Even though the tested butterfly valve has a latching device designed to fix the position of the handle and, therefore, the round disk, the tests were achieved with strictly increasing flows up to the maximum test flow and then immediately switched to a decreasing sequence of flows with the aim of detecting the effects of any possible disk displacement. This way, the position of the disk at the end of the test should be equal to or even more closed than that at the beginning, and consequently K_m should be greater or equal at the end of the test than at the beginning. A similar procedure was followed for the hydraulically operated seat globe valve, also to detect changes in position in the closing element.

For every orifice and for the two valves at every position of their closing element, the parameters K_m and $<r_{lm}$ were obtained experimentally by minimizing the minimum relative squared error defined as

$$\varepsilon_r^2 = \sum_i \min\left[\left(\frac{K_i}{K_m} - 1\right)^2 \cdot \left(\frac{\sigma_{1i}}{\sigma_{1m}} - 1\right)^2\right] \tag{20}$$

where K_t and a_u were calculated from observed data using Eqs. (2) and (3). Values are given in the figures in the Results section with $K_m \pm cr_{eKm}$ and $<r_{lm} \pm cr_{eijlm}$, where the second terms are the corresponding part of the error standard deviations from Eq. (20).

Cavitation Limits. The cavitation limit studied so far is inadequate for pipeline design purposes, and other limits such as incipient and critical cavitation limits are used. These other limits, where cavitation does not take place across the whole contracted section, will occur under less severe boundary conditions and will be positioned to the right of the curve defined by Eq. (11) for sharp-edged orifices and by Eq. (14) for valves in the respective $K_m(cr_{lm})$ diagram. Turbulence regime-specific pressure fluctuations should play a role in the process under conditions where cavitation takes place but are not strong enough to reach the intensity corresponding to $<r_{lm}$. These cavitation limits can conceivably be related to $<r_{lm}$.

Turbulence regime-specific pressure fluctuations will produce points at which vapor pressure will approximately be reached during relatively short periods, even if the mean pressure throughout the contracted section is considerably bigger than the vapor pres-

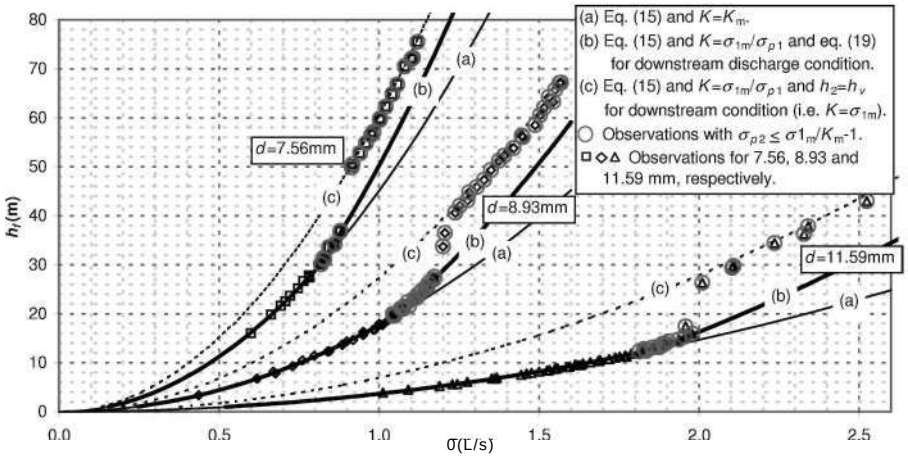

Fig. 5 Experimental and predicted results of head loss tests on sharp-edged orifices of diameter *d* in a pipe with an internal diameter D=16 mm

sure. In addition, although the root mean square values of pressure fluctuations do not vary with the jet speed, as noticed by Ran and Katz , the probability distribution changes significantly, causing a reduction in the incipient cavitation index with increasing velocity. However, considering that the pressure pulses close to the contracted section could be approximately proportional to the squared velocity pulses, as dictated by Bernoulli's equation for steady regime, for a pressure pulse intensity *p'*, the relation between a cavitation limit *cr^* with pressure fluctuation *p'* and cr_{lm} would be

$$\sigma_{1f}=\frac{p_{1f}-p_v}{\rho\frac{U^2}{2}}=\frac{p_1-p_v+p'}{\rho\frac{U^2}{2}}=\sigma_{1m}+\frac{p'}{\rho\frac{U^2}{2}}=\sigma_{1m}+\frac{c'\cdot\rho\frac{U_c^2}{2}}{\rho\frac{U^2}{2}}$$

$$=\sigma_{1m}+\frac{c'}{\left(\frac{C_c\cdot\omega_e}{\omega}\right)^2} \qquad (21)$$

In particular, for sharp-edged orifices, with the relations shown in Eqs. (7) and (8) between the section relation and the coefficients K_m and <r_{lm}, Eq. (19) expressed as a function of the latter coefficient is

$$°"l/^{=cr}lm + ^{c'}\ '(I +°"lm) \qquad (22)$$

The coefficient *c'* indicates the amplitude of the pressure fluctuation with respect to the velocity head at the contracted section for the value *cr^*.

Results and Discussion

The points in Fig. 5 show the experimental results for head losses as a function of flow in circular sharp-edged orifices placed in the 16 mm diameter pipe and with the fixed downstream boundary condition. Curves predicting the head losses according to Eq. (15) with $K=K_m$ (curves (a)) and with $K=cr_{lm}/(T_{pl}$ (curves (b) and (c)) have also been plotted. Curve (b) corresponds to the discharge condition according to Eq. (19), whereas (c) denotes the condition $h_2 = h_v$. This approximates the minimum possible pressure head in the section where the downstream pressure is measured and is equivalent to $K=cr_{lm}$. Therefore, curve (c) is an unsurpassable limit, as these results also confirm. This curve has been obtained using a_pi = \, which corresponds to the boundary condition $h_2=h_v$.

K_m and <r_{lm} values were obtained experimentally by minimizing the relative error, as shown in Eq. (20). We have circled the experimental observations in which the calculated value is a_{pl} =S cr_{lm}/K_m, indicating that cavitation should have a significant effect on *ht.*

Points plotted in Fig. 6 show the calculated *K* and crj values from the experimental observations shown in Fig. 5, and the solid lines indicate the result of Eqs. (15) and (17). Also, we have represented Eq. (11) and the experimental determinations of K_m and cr_{lm} by points alongside their coordinates. Being unique for all the boundary conditions, this representation can be used to get parameters K_m and <r_{lm}, meaning that, as far as head losses are concerned, the tested orifices have been characterized.

As shown in Fig. 5, the two parameters predict the operation of the orifices under the imposed boundary conditions, save that it is not possible to predict whether the possible vapor cavity will extend far enough to shift the downstream condition in the downstream testing pressure tap and, if it does, for what flow value it will do so.

Figure 7 shows additional experimental results carried out on the orifice of diameter *d=8.93* mm, placed in a PVC pipe with a 16.2 mm internal diameter. Both the downstream and the upstream boundary conditions were manipulated, and we found that the theoretical curves plotted in Fig. *2(b)* were confirmed experimentally. Apart from the observations and prediction curves for head losses, Fig. 7 also includes the imposed boundary conditions *hi(Q)* and *h2(Q),* and their difference *h1-h2(Q).*

The results represented by solid points are similar to those al-

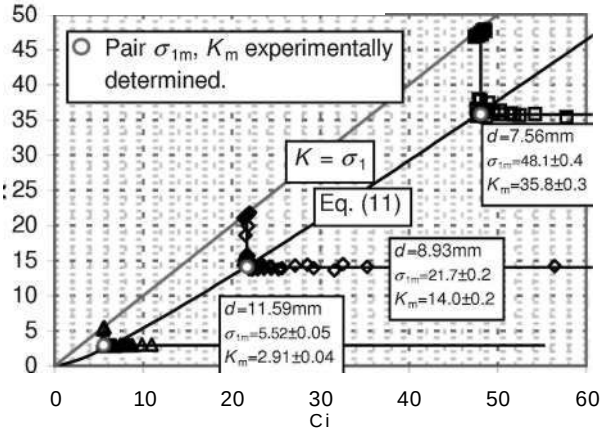

Fig. 6 Results of the proposed analysis applied to data from Fig. 5

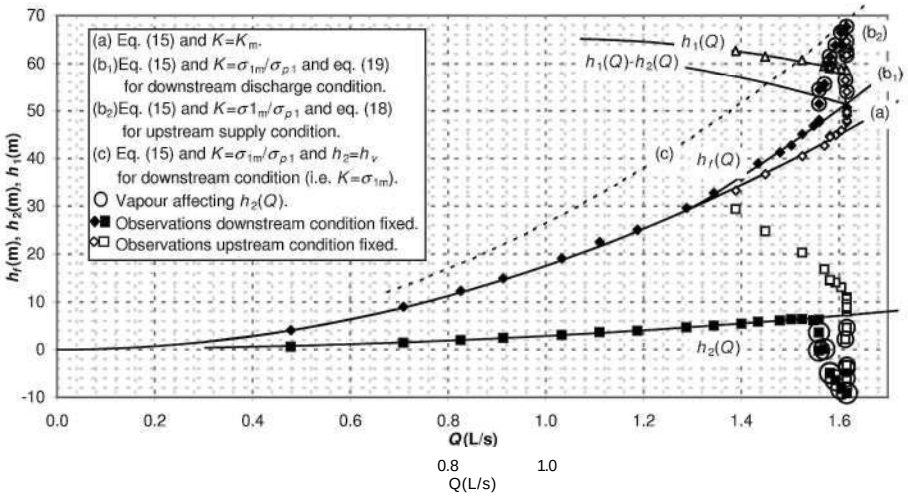

Fig. 7 Experimental results of head loss tests and predicted curves on the sharp-edged orifice of diameter d=8.93 mm in a pipe with an internal diameter D=16.2 mm

ready shown in Fig. 5, i.e., where the downstream boundary condition was constant and, particularly, V_2 was in a fully open position, whereas the empty points represent the results in which the upstream boundary condition was constant and, particularly, V_r was closed and Y_1 was in a fully open position, meaning that h_1-$h_2(Q)$ was the maximum possible head loss. The meanings of curves (a), (b), and (c) are unchanged, although (b) is now split into two: curve (bj) corresponds to the fixed downstream boundary condition and curve (b_2) corresponds to the fixed upstream boundary condition. The points that are below the line that corresponds to the imposed condition $h_2(Q)$ have been circled in Fig. 7. The explanation for this is that the vapor cavity has extended far enough to affect the measurement of the pressure difference with a manometer M_2. Note that the empty points corresponding to the fixed upstream boundary condition are still on the head loss predicting curves (a) and (b_2), whereas all the solid points are not positioned on curve (bj). The circled observations do not exactly represent the head losses, as they are above the h_1-$h_2(Q)$ curve, i.e., line (bj) does not predict that the experimental determinations do not match *ht.* However, it is clear from Fig. 8 that this topic is no longer relevant in the analysis based on the $K(<J^)$ representation, which simplifies and further specifies the determination of the parameters K_m and $<r_{lm}$. Also the points circled in Figs. 7 and 8 correspond to the same situation.

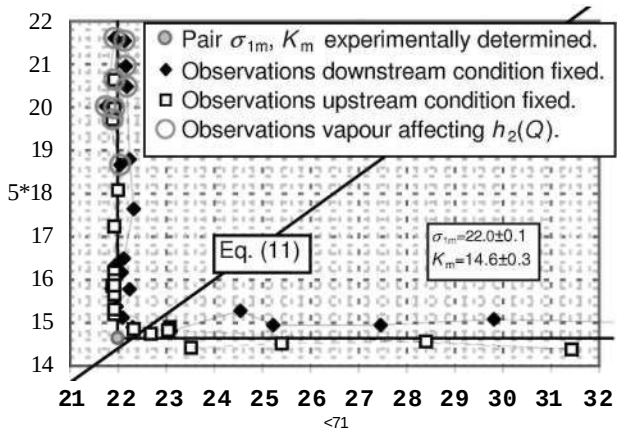

Fig. 8 Results of the proposed analysis applied to data from Fig. 7

The value of K_m obtained experimentally for the 8.93 mm diameter orifice in the 16 mm pipe was 14.0 ± 0.2, whereas it was 14.6 ± 0.3 for the 16.2 mm pipe. These results satisfy the Belanger-Borda expression shown in Eq. (8).

The points in Fig. 9 represent the experimental results of testing the butterfly valve with its round disk positioned at 45 deg. The points have been placed on two different curves, labeled as "<2 increasing" and "<2 decreasing," essentially obeying the fact that the position of the disk in the valve might change during the test. Figure 10 illustrates this more clearly. Similarly, we have plotted the curves that predict head losses according to Eq. (15) with $K = K_m$ (curves (a)) and with $K=cr_{lm}/(T_{pl}$ (curves (b)). The fitted

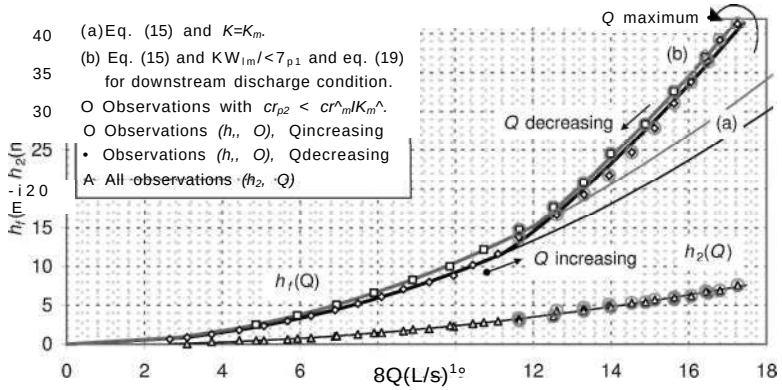

Fig. 9 Experimental and prediction results of head loss tests on a butterfly valve with a nominal diameter of 75 mm and a closing disk at 45 deg

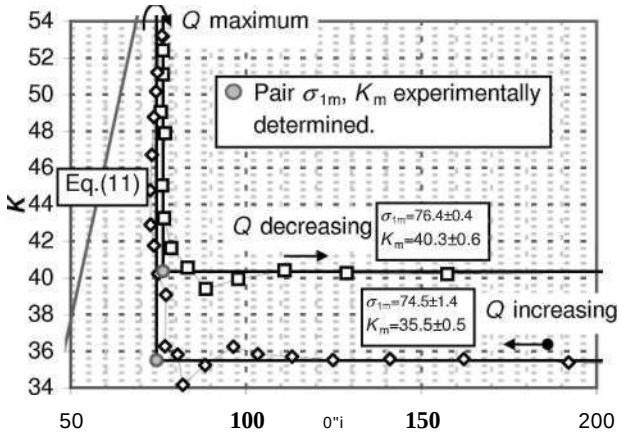

Fig. 10 Results of the proposed analysis applied to data from Fig. 9

discharge condition $h_2(Q)$ has also been represented, and unlike head losses, the observations are explained by a single curve.

As in the case of sharp-edged orifices, parameters K_m and cr_{lm} were fitted from the experimental determinations shown in Fig. 10 by minimizing the relative error shown in Eq. (20). In this case, two curves have been plotted to explain the observations for two disk positions. Accordingly, it can be said that the test started with the round disk in a position where ^"=35.5 ±0.5, and it ended with the disk in another where _fi"=40.3 ± 0.6. This change in position can be explained, bearing in mind the fact that the drag force on a disk tends to close it. Note also that according to the values of the <r_{lm} error standard deviations, the *Q* decreasing curve explains the respective experimental results slightly better than the *Q* increasing curve. This suggests that once the "<2 maximum" has been reached, the position of the disk must have been unchanged, whereas during the flow increasing phase, it must have changed in position little by little several times. This is consistent with the fact that the force on the disk, which tends to close it, will be all the greater, the greater the flow is. When that force overcomes the static friction force that keeps the disk in its place, the disk must move.

Equation (17) was also used to predict and characterize head losses in the tested butterfly valve. We found that, as was foreseeable, Eq. (11) for sharp-edged orifices does not explain the determinations of K_m and <r_{lm}, as was already mentioned in the Materials and Methods section. Experimental results fell to the right of the curve of Eq. (11), which can be interpreted as the valve got into cavitation, as far as head losses are concerned, under less severe conditions than a sharp-edged orifice with the same K_m coefficient.

Figure 11 represents the experimental determinations of K_m and cr_{lm} for several positions of the butterfly valve and the seat globe valve. Note that they are all still to the right of Eq. (11) and that a

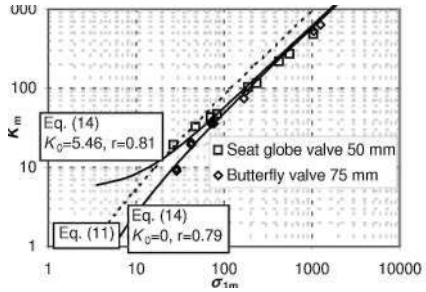

Fig. 11 Relations between experimentally determinated values of K_m and <r_{1m} on the two tested valves

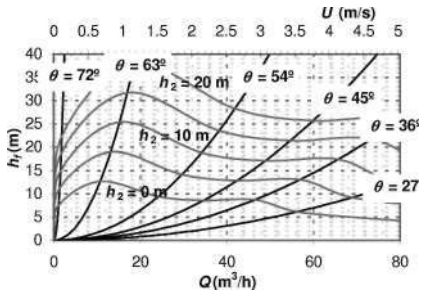

Fig. 12 Head loss curves in the tested butterfly valve for different valve positions and approximate validity bounds as a function of the downstream head pressure

value of r=0.79 with $K_0=0$, introduced in Eq. (14), would explain these values for the butterfly valve. Similarly, the coefficients r = 0.81 and K_0 = *5A6* would explain the results in the case of the seat globe valve, and not all the points are now positioned to the right of Eq. (11).

The values of the characteristic parameters can be used to elaborate the information for practical or rather "immediate" valve use, as shown in Fig. 12 for the butterfly valve. The imposed conditions have been defined in this case as a function of the downstream pressure head h_2. One point of the graph $Q(he)$ would require a downstream value of h_2 equal to the one of the curve that goes through that point plus a safety margin.

To quantify this safety margin, Eq. (21) and its particular expression for sharp-edged orifices (Eq. (22)) reflect an attempt at approximating the magnitude of the pressure pulses through the intensity or continuity of cavitation. Taking Tullis' experimental determinations about the critical and incipient cavitation limits for three sharp-edged orifices, Figs. 13 and 14 show a possible explanation based on Eq. (22). These results clearly show that as the author stated and as quantified by empirical equations, the effect of scale is patent. Besides, Arndt suggested quantifying this effect of scale on incipient cavitation by studying semiempirically the pressure drop inside a vortex produced in the wake of a disk and expressed the incipient cavitation index as a function of geometrical dimensionless parameters, Strouhal number St and Re. Also, Katz and O'Hern's results were consistent with the assumed trend of the cavitation inception index of sharp-edged bodies to increase with Re. Thus, we have adopted $c' \sim D^{0.5}$ since it has shown a reasonable agreement with the experimental results. If this approximation is accepted, apart from characterizing each singularity, the parameter <r_{lm} also serves as a reference for other less severe cavitation limits that are more useful for design purposes than <r_{lm} itself.

The above presented results for evaluating design cavitation limits are certainly limited and call for further research. In particular, it should be interesting to have at one's disposal the actual

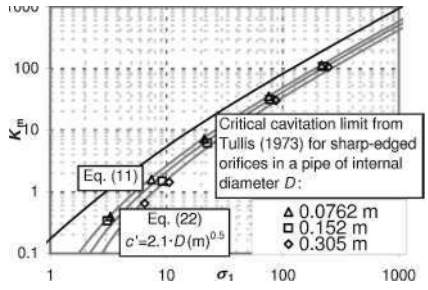

Fig. 13 Explanation of the relation between the critical cavitation limit values determined by Tullis [3] and the head loss coefficient based on the influence of the pressure fluctuation level

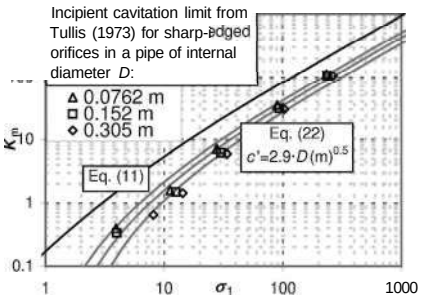

Fig. 14 Explanation of the relation between the incipient cavitation limit values determined by Tullis and the head loss coefficient based on the influence of the pressure fluctuation level

values stated by the valve's manufacturers for contrasting the proposed expressions and evaluating the coefficient *c'*.

Conclusions

Head losses under cavitating flow conditions in sudden transitions, such as valves, can be predicted because they are characterized by the parameter $<r_{lm}$, in addition to the traditional head loss parameter K_m. The latter characterizes the flow pattern downstream of the section in which cavitation takes place, whereas cr_{lm} characterizes the flow pattern upstream of this section. In principle, both parameters must be determined experimentally. Head loss formulation under cavitation flow conditions is relatively simple, so it could become extensive in a distribution network calculation software improving its results.

The proposed head loss evaluation method splits the cavitation from other effects, including the displacement of valve closing elements due to the drag force. The influence of cavitation on the head loss coefficient has been quantified. As a consequence, uncertainties about whether or not cavitation has influenced local head losses during tests are removed. Even if the vapor phase extends to the downstream pressure tap of the transition, the determination of the two parameters that characterize and quantify such head losses is not conditioned.

If the parameter K_m for a singularity is known, it is possible to approximately estimate $<r_{lm}$, or vice versa. For design purposes, this last parameter can be used to determine the maximum flow for which head losses are not affected by cavitation under certain system-imposed boundary conditions. However, as cavitation can occur even if the flow does not surpass that maximum, it is worth taking into account a given safety margin to allow for pressure fluctuations in the flow. In this respect, $<r_{lm}$ can be adopted as a reference value to estimate other cavitation levels on the basis of the pressure fluctuation-velocity head ratio.

Acknowledgment

We would like to thank the Spanish Interministry Science and Technology Board (CICYT) for its support of this work provided through Project No. AGL2004-01689/AGR.

Nomenclature

fitting coefficients for the *Q-H* curve of a pump ($L,zr^2\text{-}T,zr^5\text{-}T^2$)
c = fluctuation coefficient
c_c = contraction coefficient
c_D = discharge coefficient ($L^{5/2}\text{-}T^{-1}$)
g = gravitational acceleration ($L\text{-}T^{-2}$)
H = energy head (L)
h = pressure head (L)
h_l = head losses (L)
K = local head losses coefficient
K_0 = part of local head loss coefficient independent of the operation of the closing element in a valve
I, I', I'' = length inside the singularity (L)
p = pressure ($M\text{-}L^{-1}\text{-}T\sim^2$)
p' = pulse pressure ($M\text{-}L^{-1}\text{-}T\sim^2$)
Q = flow rate ($L\text{^}T"^1$)
r = axial-asymmetry coefficient
Re = Reynolds number
St = Strouhal number
U = mean water velocity at uniform pipe sections ($L\text{-}T"^1$)
Az = elevation difference (L)
e_r = relative error
y = specific weight ($M \bullet L\sim^2 \bullet T\sim^2$)
p = density ($M\text{-}L^{-3}$)
$<j, a_p$ = cavitation numbers
$(o$ = cross-sectional area (L^2)

Subscripts

1 = at upstream section
2 = at downstream section
c = contraction of flow
e = obstructed section
/ = fluctuating
m = minimum
ii = vapor

References

Tullis, J. P., 1981, "Modeling Cavitation for Closed Conduit Flow," J. Hydr, Div., 107(HY11), pp. 1335-1349.
Ball, J. W., and Tullis, J. P., 1973, "Cavitation in Butterfly Valves," J. Hydr. Div., 99(HY9), pp. 1303-1318.
Tullis, J. P., 1973, "Cavitation Scale Effects for Valves," Inf. Sys., 99(HY7), pp. 1109-1128.
Testud, P., Moussou, P., Hirschberg, A., and Auregan, Y., (2007), "Noise Generated by Cavitating Single-Hole and Multi-Hole Orifices in a Water Pipe," J. Fluids Struct, 23, pp. 163-189.
Zhang, Z., and Cai, J., 1999, "Compromise Orifice Geometry to Minimize Pressure Drop," J. Hydraul. Eng., 125(11), pp. 1150-1153.
Zhang, Q. Y, and Chai, B. Q., 2001, "Hydraulic Characteristics of Multistage Orifice Tunnels," J. Hydraul. Eng., 127(8), pp. 663-668.
ANSI/ISA, 2002, "Flow Equations for Sizing Control Valves," Report No. ANSI/ISA-75.01.01-2002.
Idel'cik, I. E., 1999, *Memento des pertes de charge. Coefficients de pertes de charge singulieres et de pertes de charge par frottement* (translated into French), Eyrolles, Paris (reprint of 1969 edition).
Tullis, J. P., 1971, "Choking and Super cavitating Valves," J. Hydr. Div., 97(HY12), pp. 1931-1945.
Tullis, J. P., and Govindarajan, R., 1973, "Cavitation and Size Scale Effects for Orifices," J. Hydr. Div., 99(HY3), pp. 417-430.
Mishra, C. and Peles, Y, 2005, "Cavitation in Flow Through a Micro-Orifice Inside a Silicon MicroChannel," Phys. Fluids, 17(1), p. 013601.
Sarpkaya, T., 1961, "Torque and Cavitation Characteristics of Butterfly Valves," ASME J. Appl. Mech., 28, pp. 511-518.
Nurick, W. H., 1976, "Orifice Cavitation and Its Effect on Spray Mixing." ASME Trans. J. Fluids Eng., 98, pp. 681-687.
Batchelor, G. K., 1967, *An Introduction to Fluid Dynamics*, Cambridge University Press, Cambridge, England.
Rouse, H., and Jezdinsky, V, 1966, "Fluctuation of Pressure in Conduit Expansions," J. Hydr. Div., 92(HY3), pp. 1-12.
Sanchez, R., 2006, "Caracterizacion de Llaves Hidraulicas Automaticas y Modelacion de su Funcionamiento en Sistemas de Riego," Ph.D. thesis (in Spanish), Technical University of Madrid (UPM), Madrid.
ISA, 1995, "Considerations for Evaluating Control Valve Cavitation," Report No. ISA-RP75.23-1995.
ASAE, 1999, "Procedure for Testing and Reporting Pressure Losses in Irrigation Valves," ASAE Standards, Report No. S447 DEC98.
Tullis, J. P., and Skinner, M. M., 1968, "Reducing Cavitation in Valves," J. Hydr. Div., 94(HY6), 1475-1488.
Ran, B., and Katz, J., 1994, "Pressure Fluctuations and Their Effect on Cavitation Inception within Water Jets," J. Fluid Mech., 262, pp. 223-263.
Arndt, R. E. A., 1976, "Semiempirical Analysis of Cavitation in the Wake of a Sharp-Edged Disk," ASME Trans. J. Fluids Eng., 98, pp. 560-562.
Katz, J., and O'Hern, T. J., 1986, "Cavitation in Large Scale Shear Flows," ASME Trans. J. Fluids Eng., 108, pp. 373-376.